Proceedings of the 20th International Conference on Soil Mechanics and Geotechnical Engineering– Rahman and Jaksa (Eds)

Using near-surface CPT data to predict pipeline embedment in sands

Estimation de la pénétration des oléoducs dans du sable à partir de données de pénétromètre

Fraser Bransby
Fugro Chair in Geotechnics, University of Western Australia, Australia, fraser.bransby@uwa.edu.au

Han Eng Low
Fugro Australia Marine, Fugro, Australia

Conleth O'Loughlin, Farid Bhatti & Noor Aljabury
University of Western Australia, Australia

ABSTRACT: Prediction of pipeline embedment is critical for design of offshore pipelines, risers and spools. This is because seabed reactions to in-service pipeline movements (which govern on-seabed pipeline response) are strongly dependent on embedment. Currently, methods to predict drained pipeline embedment either use modified bearing capacity methods, where it is difficult to select a representative angle of friction, or empirical methods based on limited model tests making their application to the specific soil conditions at a site problematical. Consequently, to investigate whether the near-surface profile of cone tip resistance may be used directly in design a series of cone penetrometer and pipeline monotonic penetration tests were carried out in laboratory conditions. Pipeline diameters ranging from 10 mm to 125 mm and CPTs ranging from a standard 36 mm diameter cone down to a 7 mm diameter cone were used. All tests were conducted, drained, in the top 300 mm of silica sand 'seabeds' prepared at different density states. The pipeline results confirmed that penetration resistance could be approximated using a bearing modulus approach and this could be correlated to the near-surface cone resistance.

RÉSUMÉ : La réponse des sols pulvérulents aux différents mouvements des oléoducs et conduits lors de leur opération dépends fortement de leur pénétration. L'estimation de cette pénétration est donc un paramètre essential du dimensionnement, pour laquelle les méthodes actuelles, dans le cas d'un chargement drainé, repose, soit sur la théorie de la capacite portante (avec une estimation incertaine de l'angle de friction approprié), soit sur des méthodes empiriques développées à partir d'essais de laboratoire (limitant leur application aux cas spécifiques étudiés). Des essais de laboratoire a 1g ont été réalisés afin d'évaluer la possibilité d'utiliser les résultats d'un pénétromètre pour une estimation direct de la pénétration des oléoducs. Des modèles d'oléoducs avec des diamètres de 10 à 125 mm ont été utilisés dans un sable siliceux préparés à différentes densités, conjointement à des essais pénétrométriques de diamètres 7 à 36 mm. Tous les tests ont été effectués en conditions drainées avec des pénétrations du modèle et du pénétromètre limitées à 300 mm. Les résultats indiquent qu'il est possible de prédire la pénétration du modèle en utilisant un facteur de portance corrélé aux résultats du pénétromètre près de la surface du sol.

KEYWORDS: Pipeline geotechnics, pipe-soil interaction, site investigation, cone penetration test.

1 INTRODUCTION

Prediction of pipeline embedment is critical for the design of surface-laid offshore pipelines, risers and spools. This is because seabed reactions to in-service pipeline movements are strongly dependent on embedment (e.g. Verley & Sotberg 1992, Zhang et al. 2002, Merifield et al 2008 etc.) and the response of pipelines/risers/spools to hydrodynamic loading or changes in temperature depend significantly on the amount of soil resistance acting against their movement (e.g. Bruton et al. 2008, DNV-RP-F109 2010). Furthermore, either low or high soil resistances (which are likely to correlate with low or high pipeline embedments) may govern design (e.g. White et al. 2014), and so embedment calculations should attempt to predict embedment most accurately, rather than making 'safe' over- or under-estimates.

In order to predict pipeline embedment, a core requirement is to first quantify how the vertical soil resistance per unit length of pipeline (V) increases as the pipeline penetrates vertically (w) into the seabed for the first time (see Figure 1). This relationship may be sufficient to predict the embedment of a crane-laid expansion spool (e.g. Bransby et al. 2017), but will need further modification to allow for the effect of dynamic pipelay movements (e.g. Lund 2000, Randolph and White 2008, Westgate et al. 2010a, b). Methods to quantify this additional embedment are the topic of additional research (see Bransby et al. 2020), but are not discussed further here.

For undrained soil response, there are generally accepted methods (either derived from analytical solutions or empirical correlations) that could be used to predict the resistance of the seabed against plastic penetration reasonably well (e.g. 'Model 2' in DNVGL-RP-F114 2019, Merifield et al. 2008). Consequently, the major challenge in estimating pipeline undrained plastic penetration is the accurate characterization of the seabed properties in the top 0.5 to 1 m of the seabed consistent with expected pipeline embedment. However, for drained (and partially drained) pipeline penetration there is less agreement in calculation approaches, which either use modified foundation bearing capacity methods or empiricism. This is hampered further by as-laid pipeline embedment generally being shallower in sandier materials than in (soft) clay soil, so knowledge of the seabed properties in the top 50-300 mm of the seabed is required.

Modified foundation bearing capacity methods (e.g. as recommended in DNVGL-RP-F114 2019) contain uncertainty because the circular pipeline geometry is not considered explicitly and, particularly, because the low stress levels and progressive failure of the soil during penetration of a pipeline makes selection of relevant operational angles of friction problematical.

Alternative empirical calculation methods (such as by Verley & Sotberg 1992) have been calibrated using limited input soil parameters (such as soil effective unit weight but without direct soil strength input) to fit data from model tests for a given range of pipeline and soil conditions. Consequently, their reliability in predicting seabed response accurately is limited as site-specific soil properties cannot be accounted for explicitly.

Zhang et al. (2002) introduced the use of a plastic bearing modulus (k_{vp}) to link the drained resistance (V) of a carbonate sand (per unit length of pipeline) to its vertical penetration (w):

$$\frac{V}{D} = k_{vp} w \quad (1)$$

where D is the external diameter of the pipeline. Note that $k_{vp} \equiv N_q.\gamma'$ in a simplified version of the standard Terzaghi (1943) bearing capacity equation, in which the N_γ (and N_c) term is negligible. Zhang et al (2002) suggested a value of k_{vp} = 350 kPa/m for carbonate sands based on a limited number of centrifuge model tests. However, uptake of the methodology in public domain literature is limited as selection of k_{vp} currently requires site-specific model testing.

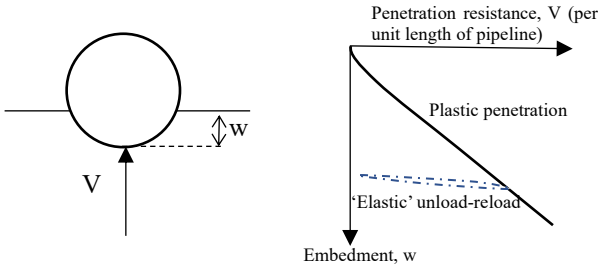

(a) Problem geometry (b) Load-resistance behaviour

Figure 1. Definition of pipe-soil interaction resistance.

Given the above difficulties, this paper investigates whether the near-surface profile of cone penetration resistance may be used directly in estimating the pipe plastic penetration in sand, in order to select a site-specific plastic bearing modulus, k_{vp}. This has the potential advantage of testing the near-surface soil in its in situ state and stress condition, without the need to take undisturbed samples (which can be problematical for coarse grained soils) and recreate the low stress conditions at the seabed surface in laboratory element testing (which is also problematical). Furthermore, the very near-surface penetration of a cone penetrometer may mobilise the soil strength in a similar manner as for pipeline penetration (e.g. Peuch & Foray 2002).

Consequently, a series of cone penetrometer and pipeline monotonic penetration tests were carried out in laboratory conditions. 'Pipelines' with diameters ranging from 10 mm to 125 mm and cone penetrometers ranging from a standard 36 mm diameter cone down to a (model scale) 7 mm diameter cone were used. All tests were conducted, drained, in the top 300 mm of dry silica sand 'seabeds' prepared at different density states.

2 EXPERIMENTAL METHODS

2.1 *Soil conditions*

The soil used for the majority of the programme was a poorly graded fine silica sand with a median grain size D_{50} = 0.18 mm and a coefficient of uniformity C_u = 1.7. It has a critical state angle of friction of 33°. Known as 'superfine silica sand' its properties are described more fully by Liu and Lehane (2012) and Chow et al. (2019).

Dry sand samples were prepared by air pluviation into sample containers (or 'strongboxes') with internal dimensions of either 1000 × 1000 × 500 mm or 800 × 400 × 1000 mm (width × breadth × depth) to achieve the desired, repeatable sample density. Strongbox samples were prepared at five different densities.

2.2 *Model pipelines and cones*

Five separate pipe segments were fabricated with diameters of 10, 25, 50, 80 and 125 mm. Each had a length six times their diameter (apart from the 125 mm pipeline which was 500 mm long), selected to reduce end effects whilst also limiting the sample footprint required. Each pipe segment was fabricated from stainless steel with a smooth (approximately 1 μm roughness) surface finish and had a 10 mm tapped thread in the middle for attachment to a load cell and actuator.

The cone penetrometers used were of diameter 7, 10, 25.4 and 35.7 mm and each had a tip load cell. The 35.7 mm cone had the standard 10 cm^2 field geometry (ISO 2014) with the smaller cones being scaled down versions of the field cone.

2.3 *Test procedure and instrumentation*

All tests were conducted with a 10 kN capacity vertical electro-mechanical actuator which was capable of penetrating the pipeline or cone penetrometer into the soil sample at a rate ranging from 0.001 to 3 mm/s. The tests reported here were conducted with dry sand so that fully drained soil response was expected for all practical penetration rates.

The vertical actuator was connected axially through an S-shaped load cell to the cone penetrometer or pipe segment being tested. Different capacity S-shaped load cells were used depending on the penetration resistance expected, but all were logged at 10 Hz during the test and were positioned to measure the total vertical soil resistance required to penetrate the device. For the CPTs, this information was augmented by load cells in each cone tip. Displacement of the device was measured by a combination of the actuator encoder (which sets the 'demand' actuator position) and vertically-oriented displacement transducers.

Once the sample had been prepared and the surface flattened by a vacuum system, the actuator and cone penetrometer or pipeline were positioned on top of the strongbox. The cone penetrometer or pipeline was initially placed above the surface of the soil to ensure that there was no soil resistance acting and so the load cell only measured the self-weight of the device (which was subtracted from the load data when obtaining the seabed resistance). The position of the device above the 'seabed' was recorded and the actuator was used to penetrate the pipeline or cone into the sample at a constant velocity (from 0.08 to 0.5 mm/s). Once the target penetration depth was achieved the cone penetrometer or pipeline was extracted vertically until the device was no longer in contact with the sample.

2.5 *Test programme*

Tests covered a range of pipeline diameters, cone diameters and sample densities. Multiple tests were conducted per strongbox sample with selection of test locations considering potential interaction between subsequent test sites.

3 RESULTS: PIPELINE PENETRATION RESISTANCE

3.1 *Pipeline penetration resistance: variation with pipeline diameter*

The typical pipeline penetration test results for a range of pipeline diameters (from 10 mm to 125 mm) in a single soil

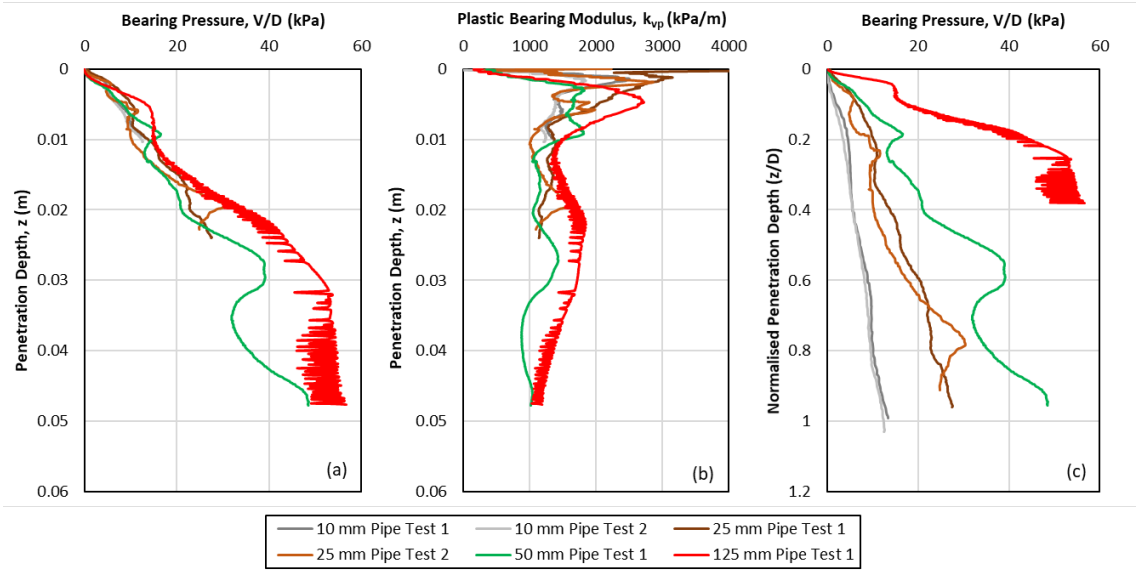

Figure 2. Pipeline resistance versus pipeline penetration for a range of pipeline diameters in dense sand (sample 1): (a) as bearing pressure (V/D) against penetration depth; (b) as bearing pressure against normalized penetration depth; (c) as bearing modulus against penetration de pth.

sample are shown in Figure 2. When the results are plotted in terms of bearing pressure (V/D) against penetration depth (z) (Figure 2a), the results from the different pipeline diameters are in general agreement (i.e. are independent of pipe diameter) suggesting that the bearing modulus approach suggested by Zhang et al. (2002) (i.e. Eq. 1) is appropriate.

Note, however, that there are some low frequency fluctuations in resistance with depth for each test (that are not apparent in the cone penetrometer data presented later). These are believed to be due to the formation (and surface emergence) of progressive shear bands during pipe penetration. This suggests that it is not solely the peak angle of friction or the critical state angle that governs pipe penetration resistance. In addition, the data presented in Fig. 2 also indicates that the 'wavelength' of the ensuing load fluctuation (which is expected to correspond to the displacement required between each generation of a new shear band) increases with the diameter of the pipeline.

The values of secant bearing modulus (k_{vp} = V/(D·z)) with depth are plotted for each test in Figure 2b. After some disparities near-surface (which are believed to be because of the difficulty in creating a perfectly flat seabed sample and identifying the contact point precisely, plus because of dividing by a small value) the results converge at approximately 1400 kPa/m for all

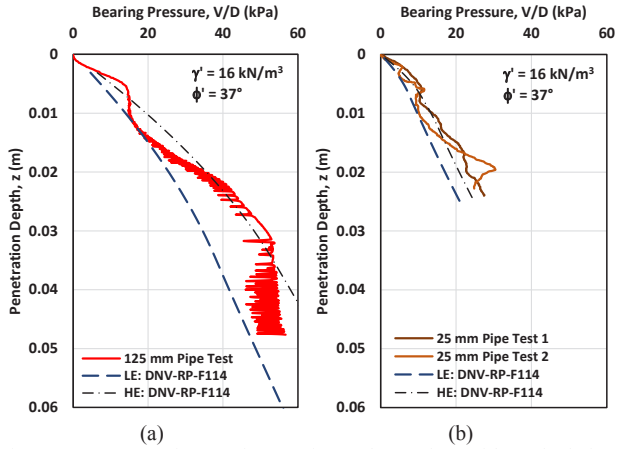

Figure 3. Comparison of experimental results with calculation approaches from DNV-RP-F109 (2010) and DNVGL-RP-114 (2019) for (a) D = 125 mm, (b) D = 25 mm.

pipeline sizes for this seabed condition after about 0.01 m of penetration. A single value of bearing modulus was selected for each pipeline test with results plotted against cone resistance (and checked for trends with pipeline diameter) in Section 5.

Pipeline penetration curves calculated from the drained penetration calculation methods recommended by DNVGL-RP-114 (2019) using soil effective unit weight (γ') of 16 kN/m^3 and soil effective friction angle (ϕ') of 37° (which is higher than the critical state friction angle of 33° for the soil sample) are shown on Figure 3 for two different pipeline diameters. Even though the predictions using this particular ϕ' agree with the measured data reasonably well, the answer on whether ϕ' should be selected based on the peak friction angle or somewhere between the peak and critical state friction angle is not definitive. Therefore, the selection of design ϕ' values for the estimation of drained pipeline penetration resistance would require engineering judgement.

3.1 *Pipeline penetration resistance: variation with soil density*

To investigate the effect of soil strength on the pipeline penetration resistance response, monotonic pipeline penetration tests were conducted in five different soil samples (each with a different density) and the plastic bearing modulus (k_{vp}) were calculated for each test. Typical results for the pipeline penetration tests conducted with 25 mm and 50 mm pipelines in seabed with a range of soil densities are plotted on Figure 4 for both pipe penetration resistance and secant bearing modulus profiles. The results presented in Figure 4 reveals the increase in pipeline penetration resistance and k_{vp} with increasing soil density (or soil strength) and smoother penetration resistance curves were observed for looser sand (because of reduced shear-banding).

4 RESULTS: CONE PENETRATION RESISTANCE

4.1 *Cone penetration resistance: variation with cone diameter*

Figure 5a shows the cone penetration resistance (q_c) profiles measured in dense sand with cone penetrometer of a range of cone diameters. Repeat tests suggested that there was a small amount of experimental variability, though this variability was less significant than the differences in results between different

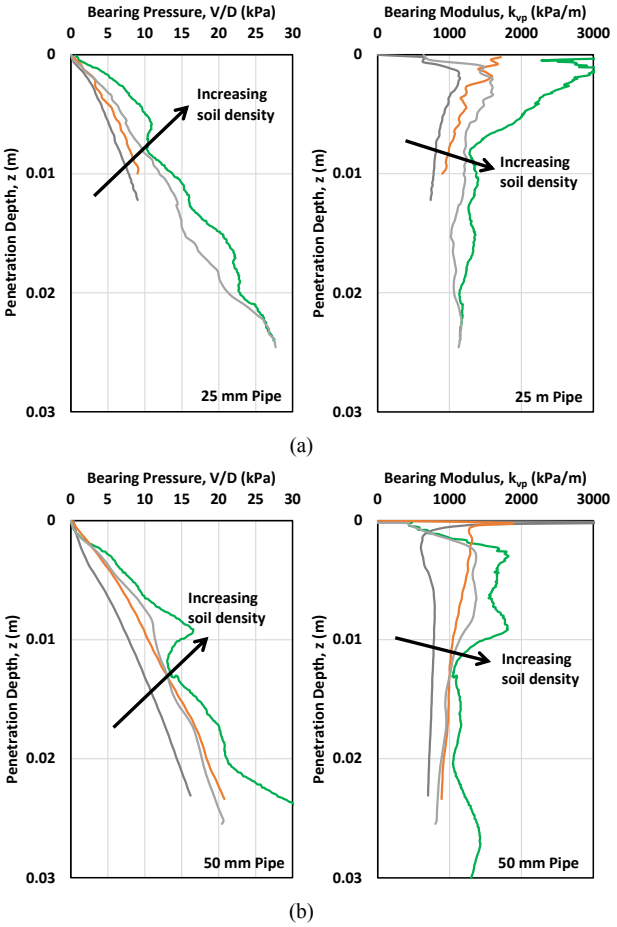

Figure 4. Pipeline penetration resistance and secant bearing modulus profiles in a range of soil densities, for (a) 25 mm pipeline and (b) 50 mm diameter pipeline.

cone sizes. It can be observed on Figure 5a that the near-surface cone resistance for the larger cones is significantly lower than for the smaller diameter cones.

The results are replotted as normalized cone penetration resistance Q_t (=q_c/σ'_v) on Figure 5b and with the depth further normalized by cone diameter in Figure 5c. Figure 5c suggests that the Q_t values for all sized cones is converging to a 'deep' cone penetration resistance (with Q_t between 300 and 400) as the (normalized) cone penetration depth increases. Consequently, the lower q_c values near the surface is because the larger cones require a proportionally larger penetration to transition from a near-surface soil deformation mechanism to a deep penetration failure mechanism.

4.2 *Cone penetration resistance: variation with soil density*

Figure 6 shows the Q_t profiles measured with cone penetrometers of various cone sizes in loose sand (Fig. 6a) and very dense sand (Fig. 6b) samples. The same trend of convergence towards a constant value of Q_t is indicated, although the data seems to suggest that a larger penetration depth is required to achieve deep penetration failure mechanism as the soil becomes denser.

4.3 *Near-surface cone penetration resistance*

Figure 7 shows the cone penetration resistance data for tests conducted with the full-size cone penetrometer (35.7 mm) and almost full-size cone penetrometer (25.4 mm). In Figure 7a, it can be seen that the cone penetration resistances measured with the two cone penetrometers are almost the same for all depths. This is confirmed by plotting the secant gradient of cone penetration resistance (q_c/z) in Figure 7b. Furthermore, the value of cone gradient for the two cone diameters converge to a fixed value (of about 1100 kPa/m) at the soil surface before increasing with depth.

If it is assumed that the failure mechanism for near surface cone penetration corresponds to that of a shallow (cylindrical) foundation and that the N_γ term of the bearing capacity is small (as suggested by Peuch & Foray, 2002), this very near-surface cone penetration resistance gradient corresponds to $q_c/z = N_q.\gamma'$.

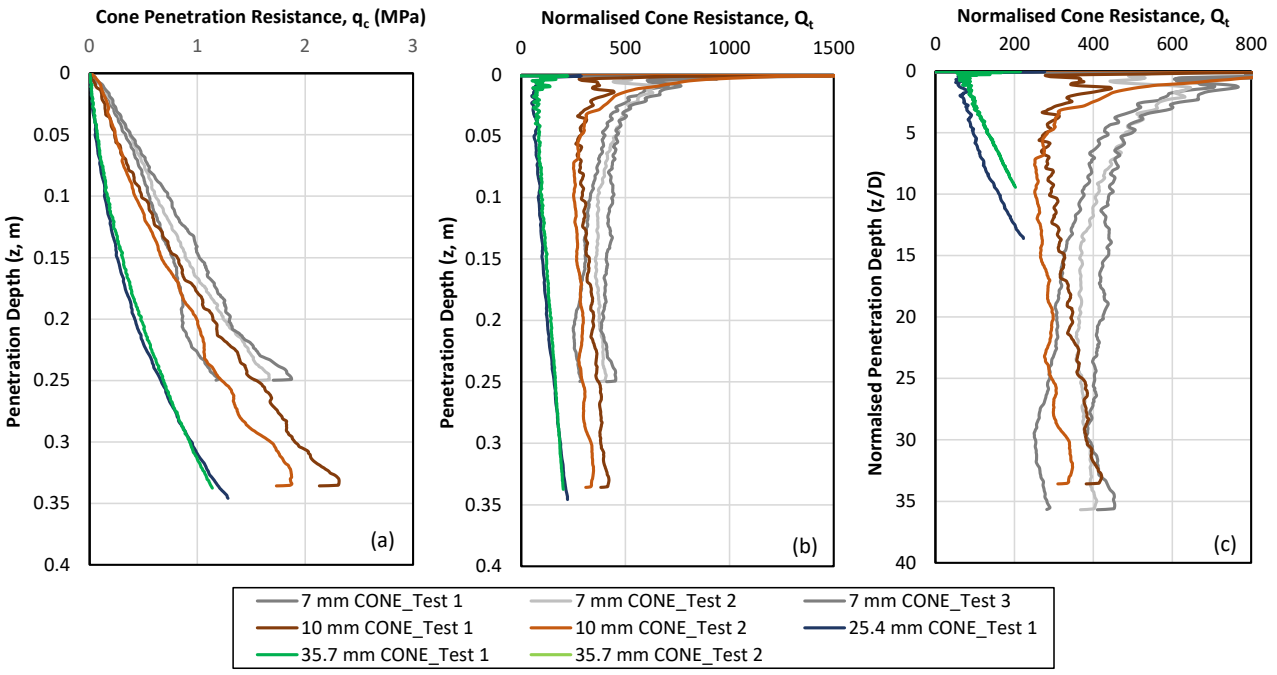

Figure 5. Cone tip resistance profiles in dense sand for a range of cone diameters: (a) cone penetration resistance against depth; (b) normalized cone resistance against depth, and (c) normalized cone resistance against normalized depth.

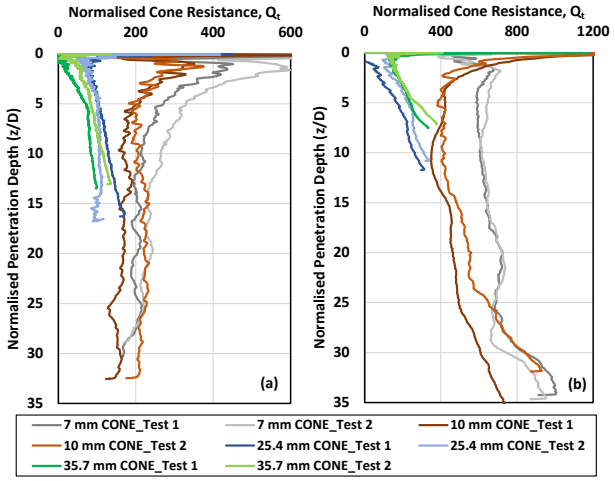

Figure 6. Normalised cone penetration resistance versus normalized pipeline penetration in (a) loose sand, and (b) very dense sand.

Taking $N_q = 1.0584e^{6.1679 \cdot \tan\phi'}$ (Peuch & Foray, 2002), a ϕ' of 34.2° and a γ' of 16 kN/m^3 is required to obtain the q_c/z of 1100 kPa/m, as observed by extrapolating the measured q_c/z (in Fig. 7b) to the soil surface.

The increase in q_c or q_c/z with depth is first expected to be due to an increase in bearing capacity as the cone tip depth to diameter ratio increases before later reaching a 'deep' cavity expansion type failure mechanism. The increase in q_c and q_c/z with depth for the shallow mechanism has been approximated by Peuch & Foray (2002) by considering an N_q mechanism, but increasing the vertical stress at the cone tip level in the equation to account for the additional resistance of the soil shearing above the cone tip as per the following equation:

$$q_c/z = \gamma' \cdot N_q \cdot (1 + K \cdot \sin\phi' \; z/L) \qquad (2)$$

where $L = D \cdot e^{\pi/2 \cdot \tan\phi'} \cdot \tan(\pi/4 + \phi'/2)$; D is the cone diameter; K is the dimensionless factor governing the friction between the cylinder an the soil at rest. A fit to the measured q_c and q_c/z data using a value of $K = 2$ (together with $\phi' = 34.2°$ selected to fit the cone surface gradient) is shown on Fig. 7 which broadly supports this interpretation.

The above interpretation suggests that it may be possible to select an operative ϕ' from near-surface cone penetration data. However, the operative ϕ' deduced from the near-surface cone penetration data (34.2°) seems to be lower than the ϕ' deduced from matching the measured pipe penetration resistance profiles with the resistance profiles estimated using the drained penetration calculation methods recommended by DNVGL-RP-114 (2019) (37°, see Section 3.1). This suggests either the operative ϕ' deduced from the near-surface cone penetration data is closer to the critical state value than expected or the N_q functions for the estimation of either near surface cone or pipe penetration resistance need modification.

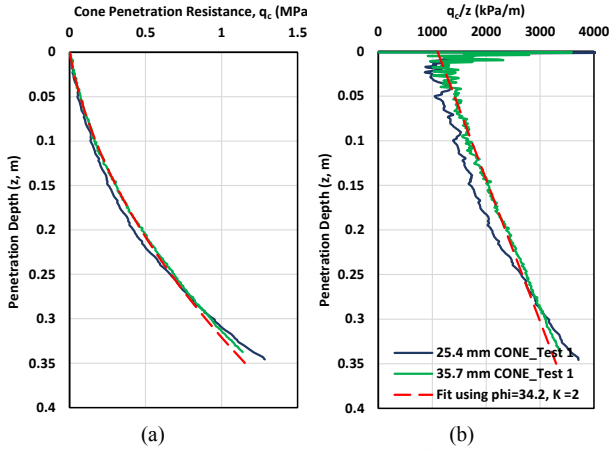

Figure 7. Cone penetration resistance data for medium-dense sample: (a) penetration resistance versus depth, (b) penetration resistance gradient versus depth.

The alternative method for selecting ϕ' for the estimation of drained pipe plastic penetration resistance could be through laboratory testing on undisturbed soil samples (but recovering high quality undisturbed sandy soil samples is a challenge by itself). Engineering judgement is then required to decide on whether the measured peak, critical state or an intermediate ϕ' should be used in calculations.

Since the pipeline and cone penetration test data presented in this paper show that both pipeline bearing modulus and cone penetration resistance are affected by sand density (or strength) in similar way, use of direct correlations between cone resistance and pipeline bearing modulus for the estimation of drained pipe plastic penetration resistance could potentially be viable and more practical and hence is explored in the following section.

5 CORRELATIONS OF CONE RESISTANCE WITH PIPELINE BEARING MODULUS

Noting that the near-surface cone penetration resistance data appears to be dependent on cone diameter, Figure 8 plots values of pipeline bearing modulus (k_{vp}) for each pipeline penetration test against the near-surface cone penetration resistance gradient (q_c/z) measured with the 25.4 and/or 35.7 mm cones only to reflect the actual cone diameters used in practice. Although the data are scattered, there is the expected trend of increasing k_{vp} with increasing q_c/z. The linear black line represents a line of best fit and thus forms a simple best estimate (BE) of the relationship. The dotted lines represent high estimate and low estimate trends located 25% above or below the BE trend.

The gradient of the best fit line shown in Figure 8 has a gradient of 0.3. This suggests that the value of q_c/z near the soil surface is much more dependent on the density (or strength) of the sand than the k_{vp} value, perhaps suggesting that a soil effective friction angle closer to the critical state friction angle is mobilized in the pipeline penetration events.

The BE trend line was used to calculate the values of k_{vp} for each pipeline penetration test and compared to the measured values. These results are plotted against cone penetration resistance gradient (in Fig. 9a) and pipeline diameter (Fig. 9b) and reveal that there is no bias in the estimation error against either of those parameters. The overall mean value of (calculated/predicted) k_{vp} value was 1.04 with a standard deviation of 0.14.

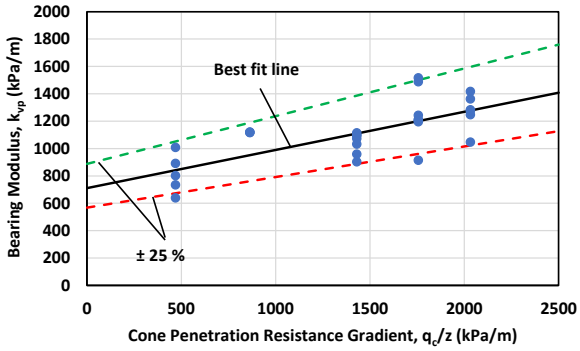

Figure 8. Correlation between near-surface cone penetration resistance gradient and measured bearing modulus (all tests)

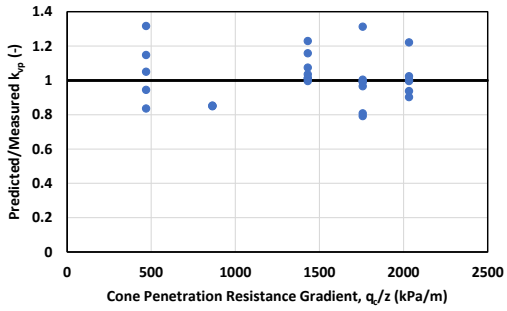

(a)

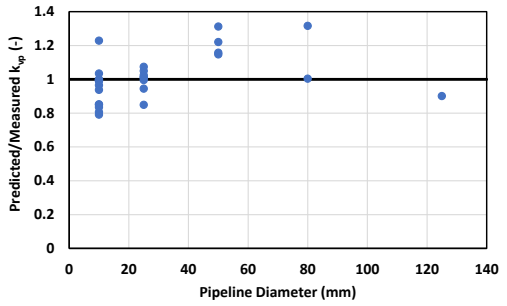

(b)

Figure 9. Accuracy of BE trend to predict pipeline bearing modulus plotted against (a) cone penetration resistance gradient, and (b) pipeline diameter.

6 IMPLICATIONS FOR DESIGN

The data presented in this paper suggest that resistance to monotonic vertical pipeline penetration into sandy seabed under drained conditions could be encapsulated using a bearing modulus approach, i.e. Eq.1, with a pipeline bearing modulus (k_{vp}) that is independent of pipeline diameter. Such an approach has only been suggested for use in carbonate sands (e.g. Zhang et al. 2002). Furthermore, it was also showed that the k_{vp} appears to correlate reasonably well with the near seabed cone penetration resistance gradient (q/z). This appears to have the potential to be a more robust method than attempting to select and use an effective friction angle for the calculation of pipeline penetration resistance, particularly because of the ubiquity of cone penetration tests (CPTs) being conducted in offshore site investigation and the difficulty of obtaining high quality intact sand samples. Therefore, the findings presented in this paper warrant further pipeline and cone penetration testing in other sandy soil types to further confirm the applicability of bearing modulus approach and the correlation between k_{vp} and q/z for the estimation of pipeline penetration resistance in other sandy soil types.

However, obtaining the value of q/z in the top few centimeters of the seabed initially appears impractical offshore where CPT data is logged at 1 Hz during a cone penetration rate of 20 mm/sec (as specified in ISO 19901-8): there is sparse data and it is difficult of accurately identify the 'zero depth' point. However, by plotting the cone gradient versus depth and extrapolating the data back to the seabed surface (as done in Fig. 5b and used in the correlations in this paper) appears to be practical and a promising approach.

7 CONCLUSIONS

The paper reports a series of pipeline penetration tests in drained silica sand, supported by cone penetrometer tests. Both the effect of cone and pipeline diameter and sand density state were investigated to allow methods for calculating monotonic pipeline penetration resistance to be evaluated and modified.

The pipeline penetration test results revealed that the variation of pipeline penetration resistance with embedment could be approximated using a bearing modulus (k_{vp}) whereby the pipeline penetration resistance (in pressure units) for a given embedment and k_{vp} were largely independent of pipeline diameter. In contrast, the CPT data revealed significant differences in near-surface cone penetration resistances measured with different cone diameters in the top 300 mm of the 'seabed', which appeared to be due to the soil deformation mechanism transition from a surface (unconstrained) to deep (constrained) mechanism which requires more penetration to mobilize deep mechanism for larger cones.

Finally, a calculation approach linking the cone penetration resistance gradient (from the near-surface data for a standard diameter cone) to the pipeline bearing modulus under monotonic vertical load has been tentatively proposed. Further testing in sandy soils with different mineralogy (such as carbonate sand) is required to validate the general applicability of this design approach.

6 ACKNOWLEDGEMENTS

The first author holds the position of the Fugro Chair in Geotechnics whose support is gratefully acknowledged.

7 REFERENCES

Bransby M.F., Low H.E., Zhu F., Clavaud R. and White, D.J. 2020. Pipe-soil interaction for surface-laid p ipelines in carbonate sediments. Proc. *ISFOG 2020*.

Bransby M.F., Ramm M., Zhou H., Low H.E. and White, D.J. 2017. Pipe-Soil Structure Interaction: Best practices for spools, buckle initiators, end connections and sand waves. In *Offshore Technology Conference*. Houston, Texas, USA.

Bruton D.A.S, White D.J., Carr M. and Cheuk J.C.Y. 2008. Pipe-soil interaction during lateral buckling and pipeline walking – the SAFEBUCK JIP. *Proc. Offshore Technology Conference*, Houston May 2008.

Chow S.H., Roy A., Herduin M., Heins E., King L., Bienen B., O'Loughlin C.D., Gaudin C. and Cassidy M.J. Characterisation of UWA superfine silica sand. Centre for Offshore Foundation Systems, Report GEO 18844.

DNV-RP-F109 2010. DNV-RP-F109. *On-bottom Stability Design of Submarine Pipelines*. DNV Recommended Practice, October 2010.

DNVGL-RP-F114 2019. DNVGL-RP-F114. *Pipe-soil interaction for submarine pipelines.* DNVGL Recommended Practice.

ISO 2014. *ISO 19901-8: Petroleum and natural gas industries — Specific requirements for offshore structures — Part 8: Marine soil investigations.* ISO copyright office, Geneva, Switzerland.

Liu, Q.B. and Lehane, B.M. 2012. The influence of particle shape on the (centrifuge) cone penetration test (CPT) end resistance in uniformly graded granular soils. *Géotechnique* 62(11), 973–984

Lund, K.M. 2000. Effect of increase in pipeline soil penetration from installation. *In Proc. of ETCE/OMAE 2000 Joint Conference*.

Merifield, R., White, D.J. and Randolph, M.F. 2008. Analysis of the undrained breakout resistance of partially embedded pipelines. *Géotechnique* 58(6), 461-470

Puech A. and Foray P. 2002. Refined model for interpreting shallow penetration CPTs in sands. *Offshore Technology Conference.* OTC 14275.

Randolph M.F. and White D. 2008. Pipeline embedment in deep water: processes and quantitative assessment. In Offshore Technology Conference. *Offshore Technology Conference*.

Terzaghi K. 1943. *Theoretical soil mechanics*. John Wiley and Sons Inc., New York, N.Y.

Verley R.L.P. and Sotberg T. 1992. A soil resistance model for pipelines placed on sandy soils. *Proc. Offshore Mechanics and Arctic Engineering Conf*, Vol V-A pipeline technology: 123–131.

Westgate Z.J., White D.J., Randolph, M.F. and Brunning, P. 2010a. Pipeline laying and embedment in soft fine-grained soils: field observations and numerical simulations, *Proc. Offshore Technology Conf*., Houston. Paper OTC 20407.

Westgate, Z.J., Randolph, M.F., White D.J. and Li, S., 2010b. The influence of seastate on as-laid pipeline embedment: a case study, *Applied Ocean Research* 32 (3), 321-331.

White D.J., Westgate Z.J. and Tian Y. 2014. Pipeline Lateral Buckling: Realistic Modeling of Geotechnical Variability and Uncertainty. *Proc. Offshore Technology Conf*., Houston, OTC25286.

Zhang, J., Stewart, D.P. and Randolph, M.F. 2002. Modeling of shallowly embedded offshore pipelines in calcareous sand. *J. Geotechnical and Geoenvironmental Engineering*, ASCE 128(5), 363–371.